GROWTH OF CARBON NANO-ONIONS IN THE OPEN AIR BY LASER RESONANT EXCITATION OF PRECURSOR MOLECULES

N305

Yang Gao[1], Jongbok Park[1], Yunshen Zhou[1], Zhiqiang Xie[1], Xiangnan He[1], and Yongfeng Lu[1]

[1] Department of Electrical Engineering, University of Nebraska-Lincoln
Lincoln, NE, 68588, USA

Abstract

In this paper, a highly efficient method was developed for the growth of CNOs in open air by effectively coupling the laser energy into the combustion flames through the resonant excitation of C_2H_4 molecules. CNOs with concentric graphitic shells were obtained at the wavelength of 10.532 μm compared with those grown without laser. The CNO growth rate at the wavelength of 10.532 μm is 2.1 g/h. Laser scattering of the CNO particles during the synthetic process indicates the formation of the CNO particles is ascribed to the direct decomposition of the C_2H_4 molecules into solid carbons on surfaces of growing particles

Introduction

Carbon nano-onions (CNOs) or onion like fullerenes are concentric multilayer giant fullerenes with concentric graphitic shells to form an encapsulated structure [1]. As important carbon-based nanomaterials together with fullerene, carbon nanotubes, and graphene, CNOs have demonstrated potential application in many fields due to their unique electronic, magnetic, optical, and tribological properties [2] such as highly delocalized π-electrons and excellent anti-wear characteristic. Up to now, researchers have reported CNO applications in gas storage [3], supercapacitors [4], broadband electromagnetic shielding [5], catalyst support in fuel cells [6], nanolubricating additives [7], environmental cleaning [2], and optical limiting [8].

In order to realize those potential applications of CNOs, one of the significant considerations is to develop a method to produce CNOs with high quality and at large quantity. Since Ugarte *et al.* [1] successfully converted carbon soot into CNOs by an intense electron beam irradiation in a high-resolution electron microscope, researchers have made their great efforts to develop various methods [2] for producing large amount of CNOs with high quality in the last two decades. However, some of these methods need high temperature and long process times (thermal annealing of diamond nanoparticles), or further steps to remove catalyst (carbon ion implantation, chemical vapor deposition). In 2004, Chio *et al.* [9] have successfully grown high-quality shell-shaped by a laser-assisted combustion process demonstrating a simple and efficient and scalable technique for growing CNOs with the production rate of 1 g/h.

In this study, a different and highly efficient laser-assisted combustion synthesis process was developed for producing CNOs in open air. Laser energy was effectively coupled into the ethylene (C_2H_4) and oxygen (O_2) combustion flame through resonant excitation of the C_2H_4 molecules using a wavelength-tunable CO_2 laser**.** In addition, no catalyst is required to form CNOs during this approach. A higher CNO growth rate approximately 2.1 g/h has been achieved. Through the resonant excitation of the CH_2 wagging mode of the C_2H_4 molecules at a wavelength of 10.532 μm, CNOs with concentric graphitic shells were obtained. Under the conditions of CNO synthesis without laser, the obtained CNOs show typical amorphous carbon structures with random and entangled graphitic layers. The effects of the vibrational energy coupling through laser resonant excitation of precursor molecules were investigated.

Experiment

Growth of CNOs was conducted in the open air by laser-assisted combustion process. Schematic diagram of the experimental setup is shown in Figure 1(a). A commercial welding torch with a 1.5 mm orifice tip was used to generate the flames. The fuel was a mixture of ethylene (C_2H_4) and oxygen (O_2) with a gas flow ratio of 5:3. A wavelength-tunable CO_2 laser (PRC, spectrum range from 9.2 to 10.9 μm) was used in the synthesis process to achieve resonant excitation of the C_2H_4 precursor molecules. Because the CH_2 wagging mode (ν_7, 949.3 cm^{-1}) of the ethylene molecules corresponding to a wavelength of 10.534 μm has a close match with the CO_2 laser line at 10.532 μm, the laser energy was coupled into the precursor molecules through resonant excitation of the C_2H_4 molecules at 10.532 μm. Silicon wafers with a dimension of 5×5×0.6 mm^3 were placed on top of the flames to collect the CNOs. The CO_2 laser tuned to

10.532 µm was directed right on the top of the nozzle and perpendicularly to the flame axis. The laser beam was focused using a ZnSe convex lens (focal length = 254 mm) to 2 mm. A typical photograph of flame without laser excitation is shown in Figure 1(b). When the laser energy was coupled into the flame at the resonant wavelength of 10.532 µm, however, the shape and luminosity of the flame had drastic changes as shown in Figure 1(c). The height of the flame was reduced as compared with the flame without laser excitation (Figure 1(b)).

Then the as-grown CNOs were characterized by a field-emission transmission electron microscope (FEI Tecnai G2 F30, 300 kV). A Renishaw inVia dispersive micro-Raman spectrometer was used to study the CNOs with a 514 nm excitation source.

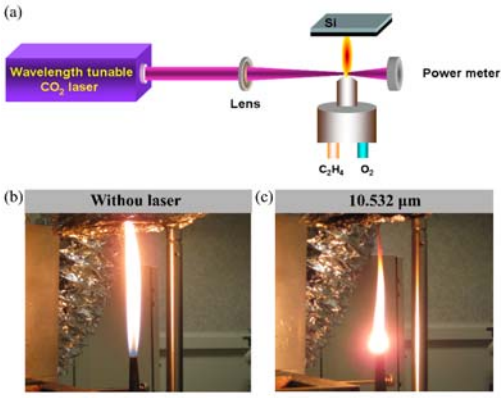

Figure 1 Illustration of the experimental setup for CNO growth with resonant excitation by a wavelength-tunable CO_2 laser. Photographs of ethylene-oxygen flames: b) without laser excitation, and c) excited at the wavelength of 10.532 µm.

Results

Figure 2 shows the SEM and TEM micrographs of CNOs grown without laser and at the wavelength of 10.532 µm. From the SEM images of CNOs grown without and with laser excitation shown in Figures 2(a) and 2(b), CNO particles agglomerate together. The size of CNOs grown without laser is larger than those grown at 10.532 µm. In Figure 2(c), the TEM image of CNOs grown without laser excitation shows typical amorphous carbon structures [10] with randomly arranged graphitic striations. For the inner part of the CNOs, the graphitic striations are entangled together; while for the outer part of the CNOs in the fringes, the graphitic striations are wrinkle-like. These wrinkle-like graphitic fringes encapsulate the inner entangled striations of the CNOs. However, CNOs grown with resonant laser energy coupling at the wavelength of 10.532 µm in Figure 2(d) demonstrate structures very different from the amorphous carbon shown in Figure 2(c). As indicated by the dashed circles, long-range ordered graphitic striations are observed to form concentric shells. The interior part of the CNOs surrounded by the concentric layers appears translucent, indicating the hollow structures of the CNOs. Additionally, through the TEM images, the diameter of the CNOs grown without laser is approximately 25 nm, while those grown at 10.532 µm have the diameter of approximately 5 nm.

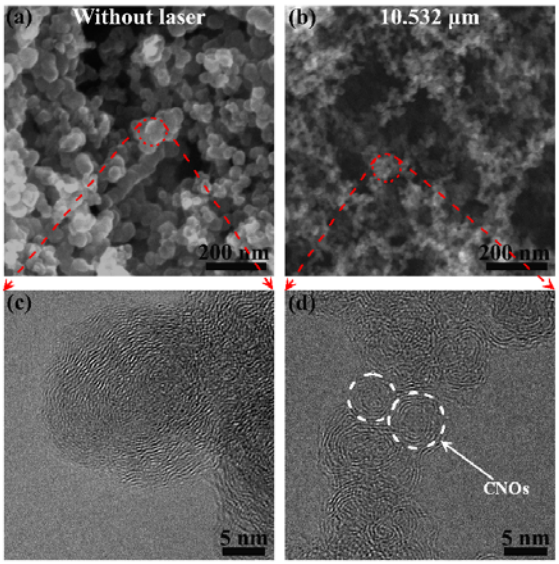

Figure 2 SEM images of CNOs grown a) without laser, b) at the wavelength of 10.532 µm. And TEM images of CNOs grown c) without laser, d) at the wavelength of 10.532 µm.

Figure 3(a) shows typical Raman spectra of CNOs grown without laser and at the wavelengths of 10.532 µm, respectively. The inset shows the magnified view of the second-order Raman peaks. In the Raman spectra, two dominant Raman shifts at 1350 and 1590 cm-1 were observed and ascribed to the D-band and G-band, respectively [11]. Due to the overlapping of the D- and G-bands, a five-band-fitting method [12] was used to study the Raman spectra. The D- and G-bands were fitted into five different bands (G, D1, D2, D3, and D4), as shown in Figure 3(b). Herein, the full width at half maximum (FWHM) of the G-bands and the relative intensities (R3= ID3/(ID3 + ID2 +IG)) of the D3 bands [11] were analyzed, as summarized in Table 1. By comparing CNOs grown under different conditions, the decreased G-band FWHM and R3 indicated the improvement in crystallinity of the CNOs prepared using a resonant excitation at 10.532 µm. The crystallinity improvement is also confirmed by the TEM study of the CNOs, which demonstrates the long-range ordered concentric graphitic shells shown in Figure 2(d). Additionally, a notable change in the second-order Raman spectra was observed. Obvious

intensity increase of the 2D-band (~2690 cm^{-1}), which is closely related to the crystallite size, further indicates the crystallinity improvement of the CNOs prepared using the 10.532 μm laser irradiation [12].

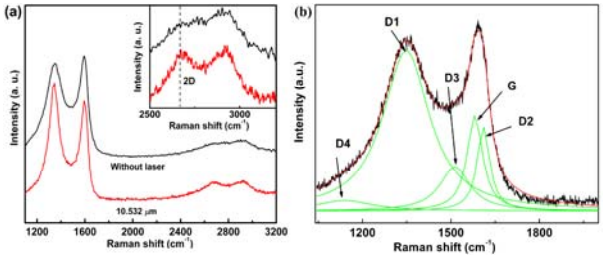

Figure 3 a) Raman spectra of CNOs grown without and at the wavelength of 10.532 μm (The inset shows the magnified view of the second-order Raman spectra). b) Typical curve fitting of the first-order Raman spectrum.

Table 1 Summary of G-band FWHM and R3 for CNOs grown without laser and at wavelengths of 10.532 μm

CNOs	FWHM of G-band (cm^{-1})	$R3=I_{D3}/(I_{D3}+I_{D2}+I_G)$
Without laser	71.4	0.24
10.532 μm	59.5	0.19

To evaluate the growth efficiency of the CNOs at the wavelength of 10.532 μm, CNO growth rate was estimated. A silicon wafer (23 mm wide × 30 mm long) was placed on top of the flames to collect the CNOs. Figure 4(a) shows the collected CNOs at the wavelength of 10.532 μm for a time period of 2 sec. The CNOs are collected in bottles as shown in Figure 4(b). CNO growth rates under different conditions are listed in Table 2. A CNO growth rate of 2.1 g/h at the wavelength of 10.532 μm was achieved, higher than those without laser excitation. Both the high growth rate and improved crystallinity of CNOs at the wavelength of 10.532 μm demonstrated that CNO growth by resonant laser excitation of C_2H_4 molecules is highly efficient.

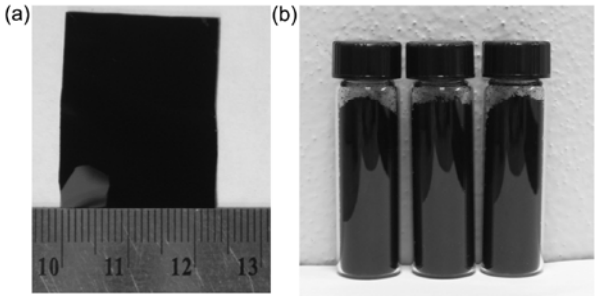

Figure 4 Photographs of collected CNOs at the wavelength of 10.532 μm a) on silicon wafer after 2 sec of deposition and b) in bottles. (0.1 g).

Table 2 CNO growth rates under different growth conditions: without laser excitation, and excitations at 10.532 μm, respectively.

	Without laser	10.532 μm
CNO growth rate	0.3 g/h	2.1 g/h

To study the growth mechanism of the CNOs with laser-assisted resonant excitation of ethylene precursor, laser scattering of the CNO particles during the growth process was conducted. The experiment setup is shown in Figure 5(a). The flame was irradiated by a Q-switched Nd:YAG laser (Powerlit precision Ⅱ 8010), which provides 6 ns optical pulses with a repetition of 10 Hz at 532 nm. An ICCD (Andor iStar DH-712) was used to take the optical images with a line filter (532 ± 10 nm) attached in the front to capture the CNO scattering light at 532 nm. From the optical images of CNO particle scattering, shown in Figure 5(b), the positions where CNOs start to grow under different conditions are identified. In the case without laser, the position starting to have obvious laser scattering from CNO particles is ~9 mm above the nozzle tip. At the wavelength of 10.532 μm, however, the distance between the nozzle tip and the position where the laser scattering from CNOs occurred decreases with the increase of the laser power, from ~9 mm at 200 W to ~7.4 mm at 1000 W.

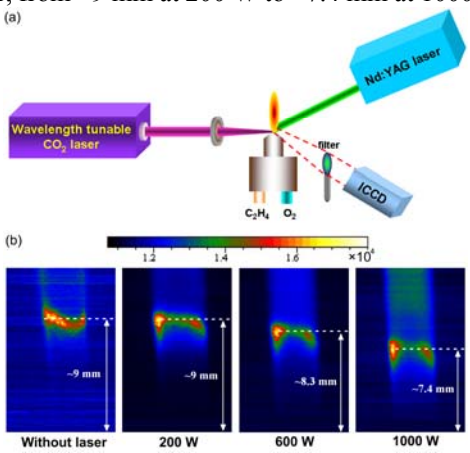

Figure 5 a) Experiment setup of laser scattering of CNO particles. b) Scattering images of CNO particles under different excitation conditions: without laser, 200, 600, and 1000 W of CO2 laser excitation at 10.532 μm.

Three possible mechanisms have been proposed to explain the formation of CNOs. The first one is similar to the carbon soot generation process, in which the polycyclic aromatic hydrocarbon (PAH) acts as the basic unit [13]. Through the process of acetylene addition and hydrogen abstraction, PAH agglomerates to form CNOs. However, since there exists variety of PAH species in the flames, continuous addition of

them onto the particle surfaces would create randomly and disconnectedly graphitic segments, which results the formation of disordered particles, or amorphous carbon, as shown in Figure 2(c). The second mechanism behind the formation of highly ordered CNOs is the restructuring of the carbon soot through bond breaking and reforming [14]. However, the CO_2 laser beam was introduced into the flames at a height of 2.5 mm to the nozzle tip, where amorphous carbon particles have not been formed, as evidenced by the laser scattering experiment. Therefore, CNOs are not formed by laser-induced restructuring of the amorphous carbons in the flame. The third mechanism proposed by Choi [9] et al. could be used to explain the experiment results. According to Choi's explanation, the heat produced in the system is proportional to the laser power and the amount of product pyrolysis. With the increase of the laser power to 1400 W, the absorbed laser energy ignites the reactions, which directly decompose acetylene precursor into solid carbons to form the shell-shaped carbon particles. In this study, laser energy is more efficiently coupled into the flame through resonant excitation at the wavelength of 10.532 μm because of the vibrational resonance. When the laser power is increased to the threshold of 400 W, the absorbed energy is sufficient to trigger the reactions instead of the high laser power required in Choi's work. Similarly, the direct decomposition of ethylene into solid carbons contributes to the formation of CNOs with the structures of long-range ordered concentric graphitic shells.

Conclusions

In conclusion, a highly efficient method was developed for the growth of CNOs in open air by effectively coupling the laser energy into the combustion flames through the resonant excitation of C2H4 molecules. CNOs grown at 10.532 μm show concentric graphitic shells, while those grown without laser show typical amorphous carbon structures. Raman spectra indicate the crystallinity improvement of the CNOs grown at 10.532 μm. The CNO production rate at the wavelength of 10.532 μm is 2.1 g/h. Laser scattering of the CNO particles during the synthetic process indicates the formation of the CNO particles is ascribed to the direct decomposition of the C2H4 molecules into solid carbons on surfaces of growing particles.

Acknowledgments

Reference

[1] Ugarte D. (1992) Curling and Closure of Graphitic Networks under Electron-Beam Irradiation, Nature 359, 707-709.

[2] Xu B. S. (2008) Prospects and research progress in nano onion-like fullerenes, New Carbon Materials 23, 289-301.

[3] Sano N., Wang H., Alexandrou I., Chhowalla M., Teo K. B. K., Amaratunga G. A. J. (2002) Properties of carbon on-ions produced by an arc discharge in water, Journal of Applied Physics 92, 2783-2788.

[4] Portet C., Yushin G., Gogotsi Y. (2007) Electrochemical performance of carbon onions, nanodiamonds, carbon black and multiwalled nanotubes in electrical double layer capacitors, Carbon 45, 2511-2518.

[5] Maksimenko S. A., Rodionova V. N., Slepyan G. Y., Karpovich V. A., Shenderova O., Walsh J., Kuznetsov V. L., Mazov I. N., Moseenkov S. I., Okotrub A. V., Lambin P. (2007) Attenuation of electromagnetic waves in onion-like carbon composites, Diamond and Related Materials 2, 1231-1235.

[6] Yang X. W., Guo J. J., Wang X. M., Liu X. G., Xu B. S. (2006) Study on characterization and growth mechanism of Pt/onion-like fullerenes catalyst, Acta Physico-Chimica Sinica 22, 967-971.

[7] Yao Y. L., Wang X. M., Guo J. J., Yang X. W., Xu B. S. (2008) Tribological property of onion-like fullerenes as lubricant additive, Materials Letters 62, 2524-2527.

[8] Koudoumas E., Kokkinaki O., Konstantaki M., Couris S., Korovin S., Detkov P., Kuznetsov V., Pimenov S., Pustovoi V. (2002) Onion-like carbon and diamond nanoparticles for optical limiting, Chemical Physics Letters 357, 336-340.

[9] Choi M., Altman I. S., Kim Y. J., Pikhitsa P. V., Lee S., Park G. S., Jeong T., Yoo J. B. (2004) Formation of shelled-shape carbon nanoparticles above a critical laser power in irridiated acetylene, Advanced Materials 16, 1721-1725.

[10] Wal L. R. V., Choi M. Y. (1999) Pulsed laser heating of soot: morphological changes, Carbon 37, 231-239.

[11] Calderon-Moreno J. M., Yoshimura M. (2001) Hydrothermal processing of high-quality multiwall nanotubes from amorphous carbon, Journal of the American Chemical Society 123,1725-1729.

[12] Sadezky A., Muckenhuber H., Grothe H., Niessner R., Poschl U. (2005) Raman microspectroscopy of soot and related carbonaceous materials: Spectral analysis and structural information, Carbon 43,1731-1742.

[13] Knauer M., Schuster M. E., Su D. S., Schlogl R., Niessner R., Ivleva N. P. (2009) Soot structure and reactivity Analysis by raman microspectroscopy, temperature-programmed oxidation, and high-resolution transmission electron microscopy, Journal of Physical Chemistry A 113, 13871-13880.

[14] Wal R. L. V., Tomasek A. J. (2004) Soot nanostructure dependence upon synthesis conditions, Combustion and Flame 136, 129-140.